A scalable and robust multigrid-based solver for the far field map of Helmholtz and Schrödinger equations

12th International Conference on Mathematical and Numerical Aspects of Wave Propagation

July 20-24 2015, Karlsruhe Institute of Technology, Germany

University of Antwerp, Applied Mathematics

S. Cools* and W. Vanroose

*Contact: siegfried.cools@uantwerp.be

Overview

[1] The Helmholtz and Schrödinger equations

[2] Classical far field map calculation for Helmholtz equations

[3] The complex contour approach for the far field map

[4] Schrödinger cross sections: the MG-CCCS preconditioner

[5] Conclusions & discussion

Motivation

Simulation of quantum mechanical molecular break-up reactions.

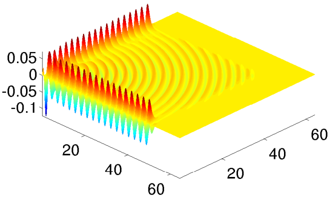

Electron wave character

CERN Large Hadron Collider

Practical use: determine material composition/structure
$\rightarrow$ inverse problem

Schrödinger equation

Full 3D break-up problem description – two particle system ($d = 2$)

Schrödinger equation (6-dimensional)

$$(\mathcal{H} - E)\,\psi(\mathbf{r}_1, \mathbf{r}_2) = \zeta(\mathbf{r}_1, \mathbf{r}_2).$$

with outgoing wave ψ i.f.o. $\mathbf{r}_1$, $\mathbf{r}_2 \in \mathbb{R}^3$ and Hamiltonian

$$\mathcal{H} = -\frac{1}{2m}\triangle_{\mathbf{r}_1} - \frac{1}{2m}\triangle_{\mathbf{r}_2} + V_1(\mathbf{r}_1) + V_2(\mathbf{r}_2) + V_{12}(\mathbf{r}_1, \mathbf{r}_2).$$

Right-hand side source term $\zeta(\mathbf{r}_1, \mathbf{r}_2)$ models

- incoming electron (electron scattering), or
  [Rescigno Baertschy Isaacs McCurdy 1999]
- dipole operator (photo-ionization).
  [Vanroose Martin Rescigno McCurdy 2005]

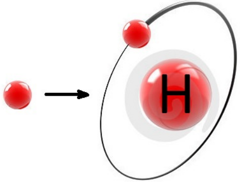

Partial wave expansion

Spherical coordinate representation: $\mathbf{r}_1 = (\rho_1, \Theta_1)$, $\mathbf{r}_2 = (\rho_2, \Theta_2)$

$$\psi(\mathbf{r}_1, \mathbf{r}_2) = \sum_{l_1=0}^{\infty} \sum_{m_1=-l_1}^{l_1} \sum_{l_2=0}^{\infty} \sum_{m_2=-l_2}^{l_2} \psi_{l_1 m_1, l_2 m_2}(\rho_1, \rho_2) Y_{l_1 m_1}(\Theta_1) Y_{l_2 m_2}(\Theta_2),$$

leads to a coupled system for the radial wave components

$$\bar{\psi} = \begin{pmatrix} \psi_{l_1 m_1, l_2 m_2}(\rho_1, \rho_2) \\ \psi_{l_1' m_1', l_2' m_2'}(\rho_1, \rho_2) \\ \vdots \end{pmatrix}$$

Coupled partial wave system

$$\begin{pmatrix} -\frac{1}{2m} \triangle_{l_1, l_2} + V_{l_1 m_1\, l_2 m_2; l_1 m_1\, l_2 m_2} - E & V_{l_1 m_1\, l_2 m_2; l_1' m_1' l_2' m_2'} & \cdots \\ V_{l_1' m_1'\, l_2' m_2'; l_1 m_1\, l_2 m_2} & -\frac{1}{2m} \triangle_{l_1', l_2'} + V_{l_1' m_1'\, l_2' m_2'; l_1' m_1' l_2' m_2'} - E & \cdots \\ \vdots & \vdots & \ddots \end{pmatrix} \bar{\psi} = \bar{\zeta}.$$

Note: system decouples for V_1, V_2 and V_{12} spherically symmetric.

Relation to Helmholtz equation

Diagonal blocks assume form of 2D driven Schrödinger equation

$$\left(-\frac{1}{2}\triangle + V(\mathbf{x}) - E\right) u(\mathbf{x}) = g(\mathbf{x}), \qquad \mathbf{x} = (x, y) \in \mathbb{R}^2.$$

Helmholtz equation (d-dimensional) *(equivalent formulation)*

$$\left(-\triangle - k^2(\mathbf{x})\right)\, u(\mathbf{x}) = f(\mathbf{x}), \qquad \mathbf{x} \in \mathbb{R}^d,$$

with $k^2(\mathbf{x}) = 2(E - V(\mathbf{x}))$ *and* $f(\mathbf{x}) = 2g(\mathbf{x})$.

Properties.

- potential $V(\mathbf{x})$ – and hence wavenumber $k(\mathbf{x})$ – is analytic,
- experimental observations (cross sections) are far field maps.
  [McCurdy Baertschy Rescigno 2004]

Helmholtz equation

Representation of the physics behind a wave scattering at an object χ defined on a compact area O located within a domain $\Omega \subset \mathbb{R}^d$.

Scattered wave solution $u_{sc}(\mathbf{x})$ satisfies inhomogeneous Helmholtz

$$\left(-\triangle - k^2(\mathbf{x})\right) u_{sc}(\mathbf{x}) = f(\mathbf{x}), \qquad \mathbf{x} \in \Omega \subset \mathbb{R}^d,$$

with $f(\mathbf{x}) = k_0^2 \chi(\mathbf{x}) u_{in}(\mathbf{x})$.

Aim: calculate far field amplitude map

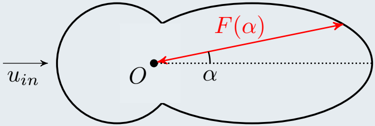

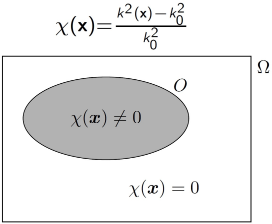

Far field map

Analytic solution on whole $\mathbb{R}^d$ using Green's function:

$$u(\mathbf{x}') = \int_\Omega \underbrace{G(\mathbf{x}, \mathbf{x}')}_{\text{Green's function}} k_0^2 \chi(\mathbf{x}) \left[u_{in}(\mathbf{x}) + \underbrace{u_{sc}(\mathbf{x})}_{\text{scattered wave}}\right] d\mathbf{x}, \quad \mathbf{x}' \in \mathbb{R}^d.$$

[Colton Kress 1998]

Calculate u in any point $\mathbf{x}' \in \mathbb{R}^d$ outside the numerical domain Ω, using only the information inside the numerical domain.

Computation: Split the far field integral into a sum $I_1 + I_2$, with

$$I_1 = \underbrace{\int_\Omega G(\mathbf{x}, \mathbf{x}') \chi(\mathbf{x}) u_{in}(\mathbf{x}) d\mathbf{x}}_{\text{all factors known explicitly}} \quad \text{and} \quad I_2 = \underbrace{\int_\Omega G(\mathbf{x}, \mathbf{x}') \chi(\mathbf{x}) u_{sc}(\mathbf{x}) d\mathbf{x}}_{\text{requires } u_{sc}(\mathbf{x}) \text{ for } x \in \Omega}$$

Preconditioned Krylov methods

State-of-the-art Helmholtz solvers.

Solve $\mathcal{M}^{-1}\mathcal{A}u = \mathcal{M}^{-1}f$ *using Krylov methods, with*

$$\mathcal{M} = -\triangle - \varrho k(\mathbf{x})^2 \qquad \textit{(preconditioner)}$$

where $\mathcal{A} = -\triangle - k(\mathbf{x})^2$ *and* $\mathcal{M}u = f$ *easily solvable iteratively.*

- $\varrho = 1$: original Helmholtz operator
  [von Helmholtz 19th century]
- $\varrho = 0$: Laplacian
  [Bayliss Goldstein Turkel 1983]
- $\varrho < 0$: shifted Laplacian or screened Poisson operator
  [Laird 2001]
- $\varrho \in \mathbb{C}$: complex shifted Laplacian (CSL): $\varrho = \alpha + \beta i$
  [Erlangga Vuik Oosterlee 2004]

Far field map

Complex contour approach.

For u and χ analytical
the far field integral

$$I_2 = \int_\Omega G(\mathbf{x}, \mathbf{x}')\chi(\mathbf{x})u_{sc}(\mathbf{x})d\mathbf{x}$$

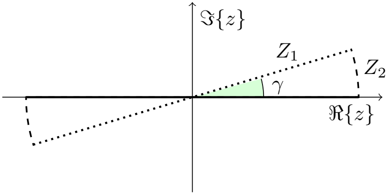

can be calculated over a *complex contour* $Z = Z_1 + Z_2$, rather than over the real domain Ω, i.e.

$$I_2 = \int_{Z_1} G(\mathbf{z}, \mathbf{z}')\chi(\mathbf{z})u_{sc}(\mathbf{z})d\mathbf{z} \; + \; \int_{Z_2} G(\mathbf{z}, \mathbf{z}')\chi(\mathbf{z})u_{sc}(\mathbf{z})d\mathbf{z}.$$

Far field map

Complex contour approach.

For u and χ analytical
the far field integral

$$I_2 = \int_{\Omega} G(\mathbf{x}, \mathbf{x}')\chi(\mathbf{x})u_{sc}(\mathbf{x})d\mathbf{x}$$

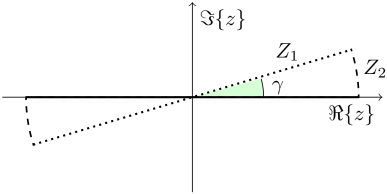

can be calculated over a *complex contour* $Z = Z_1 + Z_2$, rather than over the real domain Ω, i.e.

$$I_2 = \underbrace{\int_{Z_1} G(\mathbf{z}, \mathbf{z}')\chi(\mathbf{z})u_{sc}(\mathbf{z})d\mathbf{z}}_{\text{requires } u_{sc}(\mathbf{z}) \text{ for } \mathbf{z} \in Z_1} + \int_{Z_2} G(\mathbf{z}, \mathbf{z}')\chi(\mathbf{z})u_{sc}(\mathbf{z})d\mathbf{z}.$$

Helmholtz on complex contour

Complex shifted Laplacian (CSL) system with shift parameter $\beta \in \mathbb{R}$

$$\left(-\triangle - (1 + i\beta)k^2(\mathbf{x})\right) u(\mathbf{x}) = f(\mathbf{x})$$

is efficiently solvable using multigrid. *[Erlangga Oosterlee Vuik 2004]*

FD discretization:

$$\left(-\frac{1}{h^2} L - (1 + i\beta)k^2\right) u_h = f_h,$$

with Laplacian stencil matrix L. Division by $(1 + i\beta)$ yields

$$\left(-\frac{1}{(1 + i\beta)h^2} L - k^2\right) u_h = \frac{f_h}{1 + i\beta},$$

the original Helmholtz system with complex $\tilde{h} = \sqrt{1 + i\beta}\, h = \rho e^{i\gamma} h$.

[Reps Vanroose bin Zubair 2010]

Contour approach - 2D validation

Object of interest

5-point FD stencil, $n_x \times n_y = 256^2$

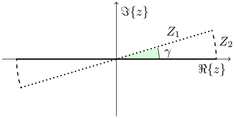

Real domain with ECS $|\chi(\mathbf{x})|$ ($\theta_{ECS} = 45^\circ$)

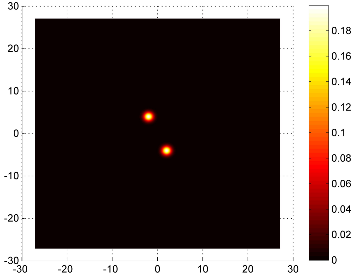

Complex contour $|\chi(\mathbf{z})|$ ($\gamma = 14.6^\circ$)

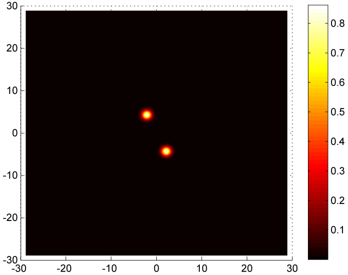

Contour approach - 2D validation

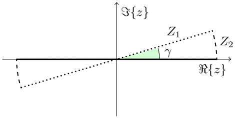

Scattered wave solution

5-point FD stencil, $n_x \times n_y = 256^2$

Real domain with ECS $|u(\mathbf{x})|$
LU factorization

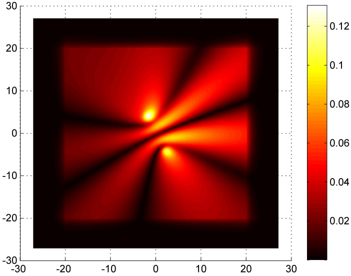

Complex contour $|u(\mathbf{z})|$
V(1,1) cycles ($tol_{res} = 10^{-6}$)

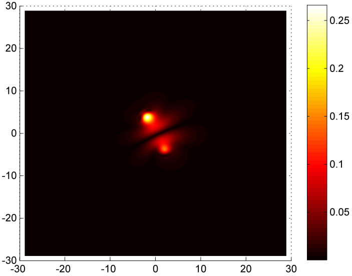

Contour approach - 2D validation

Far field amplitude map

5-point FD stencil, $n_x \times n_y = 256^2$

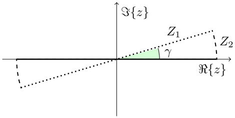

Real domain with ECS $F(\alpha)$
LU factorization

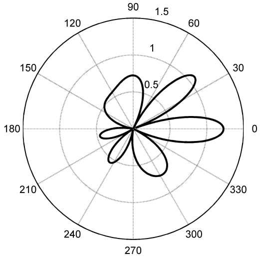

Complex contour $F(\alpha)$
V(1,1) cycles ($tol_{res} = 10^{-6}$)

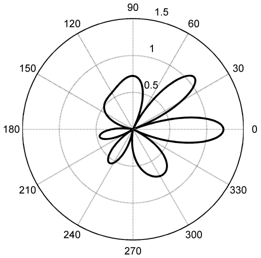

Contour approach - 3D validation

3D damped Helmholtz solver ($\gamma = 10^\circ$)

$n_x \times n_y \times n_z$	16^3	32^3	64^3	128^3	256^3
$k_0 = 1/4$	**10** (0.79s.) 0.24	**9** (4.65s.) 0.20	**9** (44.2s.) 0.21	**9** (352s.) 0.20	**9** (2778s.) 0.20
$k_0 = 1/2$	12 (0.92s.) 0.31	**10** (4.96s.) 0.24	**10** (48.3s.) 0.22	**10** (390s.) 0.23	**9** (2797s.) 0.21
$k_0 = 1$	7 (0.62s.) 0.13	13 (6.59s.) 0.32	**11** (54.6s.) 0.27	**10** (387s.) 0.24	**10** (3079s.) 0.24
$k_0 = 2$	2 (0.28s.) 0.00	8 (4.24s.) 0.14	13 (63.9s.) 0.33	**11** (428s.) 0.27	**10** (3006s.) 0.24
$k_0 = 4$	1 (0.20s.) 0.00	2 (1.35s.) 0.00	7 (36.1s.) 0.12	13 (503s.) 0.33	**11** (3306s.) 0.26

GMRES(3)-smoothed V(1,1) cycles ($tol_{res} = 10^{-6}$) $k_0 h = 0.625$

Contour approach - 3D validation

3D damped Helmholtz solver ($\gamma = 10^\circ$, $k_0 = 1$)

$n_x \times n_y \times n_z$	16^3	32^3	64^3	128^3	256^3
CPU time	0.20 s.	0.78 s.	6.24 s.	53.3 s.	462 s.
$\|r\|_2$	3.3e-5	7.9e-5	2.7e-5	1.1e-5	4.6e-6

GMRES(3)-smoothed FMG(1,1) cycle

256^3
8×573 s.
1.0e-5

[Vasseur 2012]

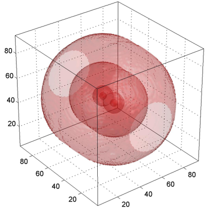

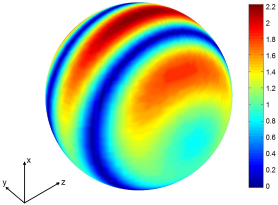

Serial implementation, Intel Core i7-2720QM 2.20GHz CPU, 6MB Cache, 8GB RAM.

Schrödinger cross sections

Single ionization amplitude *(single ionization probability)*

$$s_n(E) = \int_\Omega \underbrace{\phi_{k_n}(x)\phi_n(y)}_{\text{Green's function}} \left[g(x,y) - V_{12}(x,y)\underbrace{u(x,y)}_{\text{scattered wave}}\right] dx\, dy.$$

Double ionization cross section *(double ionization probability)*

$$d_{k_1,k_2}(E) = \int_\Omega \underbrace{\phi_{k_1}(x)\phi_{k_2}(y)}_{\text{Green's function}} \left[g(x,y) - V_{12}(x,y)\underbrace{u(x,y)}_{\text{scattered wave}}\right] dx\, dy.$$

Single ionization

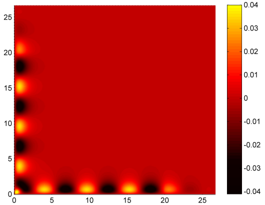

Double ionization

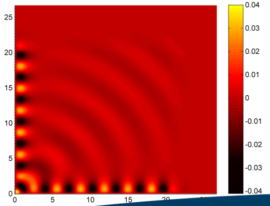

Schrödinger on complex contour

2D driven Schrödinger equation

$$\left(-\frac{1}{2}\triangle + V_1(x) + V_2(y) + V_{12}(x,y) - E\right) u(x,y) = f(x,y),$$

with $x, y \geq 0$, V_i potentials, $E \in \mathbb{R}$ energy of the system.

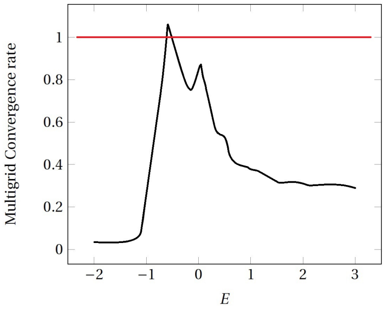

Multigrid convergence factor

- damped Schrödinger on full complex grid with $\gamma \approx 8.5°$
- GMRES(3)-smoothed multigrid V(1,1) cycles

Observation:
Poor convergence for $-1 < E < 0$.

Schrödinger spectral analysis

Single ionization		**Double ionization**
$E < 0$	$E = 0$	$E > 0$

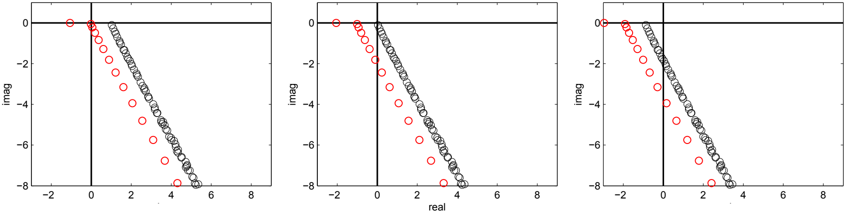

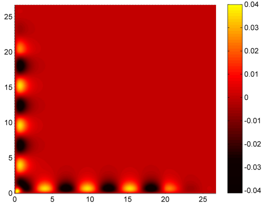

bound states
with near-zero e.v.'s
destroy multigrid
convergence

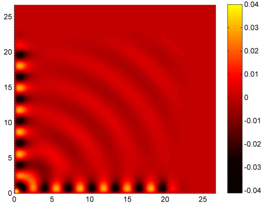

Coupled channel approximation

Bound states are characterized by eigenstates of 1D Hamiltonians

$$H_1\phi_n(x) = \lambda_n\phi_n(x),$$
$$H_2\varphi_n(y) = \mu_n\varphi_n(y),$$

with $\lambda_n < 0$ and $\mu_n < 0$, hence for $M \ll n_x$, $L \ll n_y$ approximate

$$u(x,y) \approx \sum_{m=1}^{M} A_m(y)\phi_m(x) + \sum_{l=1}^{L} B_l(x)\varphi_l(y).$$

[Heller Reinhardt 1973] [McCarthy Stelbovics 1983]

Coupled channel correction step (CCCS).

$$u^{(k+1)}(x,y) = u^{(k)}(x,y) + \sum_{m=1}^{M} e_m^A(y)\phi_m(x) + \sum_{l=1}^{L} e_l^B(x)\varphi_l(y).$$

Determine coefficients as solution of M+L 1D Schrödinger systems.

Numerical results: convergence

Convergence rate of MG-CCCS as stand-alone solver/preconditioner

Exponential model problem

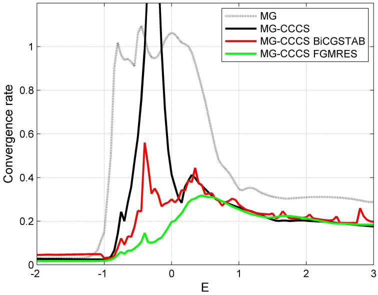

$$V_1(x) = -4.5\exp(-x^2)$$
$$V_{12}(x,y) = 2\exp(-0.1(x+y)^2)$$
$$\Omega = [0,20]^2,\ n_x \times n_y = 256 \times 256$$

Temkin-Poet model problem

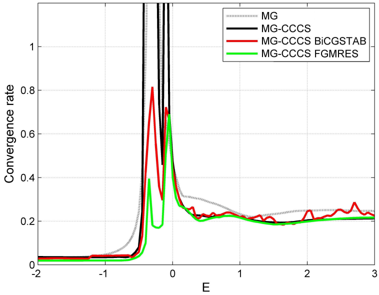

$$V_1(x) = -1/x$$
$$V_{12}(x,y) = 1/\max(x,y)$$
$$\Omega = [0,100]^2,\ n_x \times n_y = 1024 \times 1024$$

Numerical results: cross sections

2D Temkin Poet model problem

Potentials: $V_1(x) = -1/x,\ V_2(y) = -1/y$ and $V_{12}(x,y) = 1/\max(x,y)$

Discretization: $\Omega = [0,108]^2$ with $n_x \times n_y = 269 \times 269$ spectral element grid

Solver: LU with $\theta_{ECS} = 30^\circ$ (real) vs. MG-CCCS with $\gamma = 9^\circ$ (complex)

Single differential cross section

$E = 1$

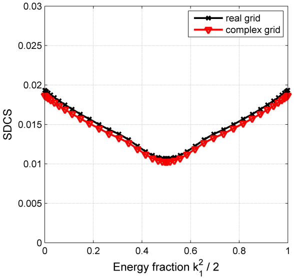

Total cross section

$E \in [0,2]$

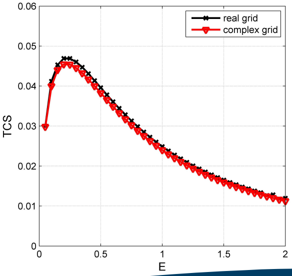

Conclusions

In this work we presented...

- ⋆ Proof-of-concept for complex contour approach to compute the far field map of Helmholtz and Schrödinger equations.
- ⋆ Fast and robust method for the computation of the far field map/ ionization cross sections for any wavenumber/energy.
- ⋆ Coupled Channel Correction Step (CCCS) after each MG V-cycle accounts for presence of localized bound states (Schrödinger).
- ⋆ Numerical validation on model problems shows $\mathcal{O}(N)$ scalability.

Outlook

- ⋆ Application of complex contour method to near field calculation.
- ⋆ Generalization to 3D Schrödinger partial wave systems.
- ⋆ Analysis of bound states and influence of complex rotation γ for general discretizations.

References

- Y.A. Erlangga, C.W. Oosterlee, and C. Vuik, *A novel multigrid based preconditioner for heterogeneous Helmholtz problems*, SIAM Journal on Scientific Computing 27(4), pp. 1471-1492, 2006.
- W. Vanroose, D.A. Horner, F. Martin, T.N. Rescigno and C.W. McCurdy. Double photoionization of aligned molecular hydrogen. Physical Review A, 74(5), pp. 052702-1-19, 2006.
- O.G. Ernst and M.J. Gander, *Why it is difficult to solve Helmholtz problems with classical iterative methods*, Numerical Analysis of Multiscale Problems, pp. 325-363, 2012.
- S. Cools, B. Reps and W. Vanroose, *An efficient multigrid method calculation of the far field map for Helmholtz problems*, SIAM Journal on Scientific Computing 36(3), pp. B367-B395, 2014.
- S. Cools and W. Vanroose, *A fast and robust computational method for the ionization cross sections of the driven Schrödinger equation using an O(N) multigrid-based scheme*, under review, arxiv:1412.1953, 2015.